

Liposome-Indocyanine Green Nanoprobes for Optical Labeling and Tracking of Human Mesenchymal Stem Cells Post-Transplantation In Vivo

Mariarosa Mazza, Neus Lozano, Debora Braga Vieira, Maurizio Buggio, Cay Kielty, and Kostas Kostarelos*

Direct labeling of human mesenchymal stem cells (hMSC) prior to transplantation provides a means to track cells after administration and it is a powerful tool for the assessment of new cell-based therapies. Biocompatible nanoprobes consisting of liposome-indocyanine green hybrid vesicles (liposome-ICG) are used to safely label hMSC. Labeled hMSC recapitulating a 3D cellular environment is transplanted as spheroids subcutaneously and intracranially in athymic nude mice. Cells emit a strong NIR signal used for tracking post-transplantation with the IVIS imaging system up to 2 weeks (subcutaneous) and 1 week (intracranial). The transplanted stem cells are imaged in situ after engraftment deep in the brain up to 1 week in living animals using optical imaging techniques and without the need to genetically modify the cells. This method is proposed for efficient, nontoxic direct cell labeling for the preclinical assessment of cell-based therapies and the design of clinical trials, and potentially for localization of the cell engraftment after transplantation into patients.

Human mesenchymal stromal cells (hMSC) have therapeutic potential for cell-based therapies by transplantation, especially for the treatment of morbidities in organs with limited regeneration capacity, such as heart and brain.^[1] Currently there are 40 clinical trials investigating the use of hMSC in brain diseases and 52 in cardiovascular conditions (excluding studies with unknown status; Clinical trial.gov database accessed 06/01/2017). Two of the challenges to successful therapy include the currently suboptimal methods in the delivery of hMSC within target tissues and the poor understanding of the in vivo fate of the transplanted cells.

The ability to monitor the fate of transplanted cells by noninvasive imaging enables the development of improved cell-based

therapies, as it allows cell tracking in host tissue microenvironments and informs on engraftment efficiency. It can also shed light on the safety of engrafted cells by monitoring their biodistribution. Labeling of hMSC before transplantation could enable tracking of cells after administration and would thus be a powerful tool for the assessment of cell-based therapies, design of clinical trials, and monitoring in clinical practice.^[2,3] At the preclinical stage, labeled cells might be recovered and analyzed to answer fundamental questions about tissue microenvironmental influences on their differentiation and integration.

Single-photon emission computerized tomography (SPECT) and positron emission tomography (PET), the most frequently used techniques to track cells, have revealed that with current delivery

methods, such as intravenous injection, cell retention is very low.^[4] Magnetic Resonance Imaging (MRI) has also been used because of its high resolution capacity, however cells need to be labeled with superparamagnetic iron oxide nanoparticles particles, and as a consequence false positive signal for cell survival or engraftment can occur because resident macrophages can take up particles leaking after cell death.^[5] Near-infrared (NIR) whole-body imaging combines low background noise with deep tissue penetration^[6] and, combined with direct labeling of stem cells prior to transplantation, can be suitable for noninvasive assessment of engraftment and tissue distribution in vivo. Nanoparticles based on different materials with outstanding optical properties in the NIR region are currently investigated to exploit the advantages of NIR whole-body imaging for stem cell tracking, such as nanodots,^[7] semiconducting polymers,^[8] gold nanodots.^[9]

We aimed to develop liposome-based NIR nanoprobes to achieve imaging with deep tissue penetration using a biocompatible, safe and nontoxic formulation. Formulations based on therapeutic liposomes-indocyanine green (ICG) have been developed for combinatory therapeutic-diagnostic applications.^[10,11] ICG is a NIR dye approved by the Food And Drug Administration (FDA), strongly photoabsorbent/fluorescent probe in the NIR optical window, with common application in ophthalmic angiography, cardiology, and hepatology,^[12] as such clinical systems designed for NIR biomedical imaging are

Dr. M. Mazza, Dr. N. Lozano, Dr. D. B. Vieira, Dr. M. Buggio,
Prof. K. Kostarelos
Nanomedicine Lab
Faculty of Biology, Medicine and Health
University of Manchester
Manchester M13 9PT, UK
E-mail: kostas.kostarelos@manchester.ac.uk
Prof. C. Kielty
Wellcome Trust Centre for Cell-Matrix Research
Faculty of Biology, Medicine and Health
University of Manchester
Manchester M13 9PT, UK

DOI: 10.1002/adhm.201700374

commercially available. By formulating ICG into liposomes, we aimed to achieve long-lasting labeling of hMSC for in vivo tracking with a noninvasive imaging optical technique, without influencing the normal cell function and eliminating the need for injection of radiolabeled contrast agents or genetic modification.

3D spheroidal cultures of hMSC are regarded as more physiological, and they have been reported to enhance paracrine secretion of angiogenic, antitumorigenic, and pro- and anti-inflammatory factors, to improve cell survival, and to increase differentiation potentials.^[13] Using liposome-labeling, we demonstrated that hMSC spheroids engrafted into subcutaneous or brain tissues were retained for at least 2 weeks, even better in some of the transplanted animals for up to 3 weeks. Incorporating this approach into studies of cell transplantation in animals and humans will be critical for the successful implementation of cell-based therapies into the clinics.

Characterization of Liposome-ICG Nanoprobes: Cationic liposomes formed by DOTAP:Chol ($2 \times 10^{-3} \text{ M} : 1 \times 10^{-3} \text{ M}$) containing $80 \times 10^{-6} \text{ M}$ ICG (liposome-ICG) were prepared using the film hydration and sonication method (Figure 1A). Transmission electron microscopy (TEM) of the liposome-ICG (Figure 1B) verified the formation of unilamellar liposomes of a mean diameter consistent with that obtained with dynamic light scattering centered at 100 nm (Figure 1C). The ζ -potential measurements (Figure 1D) corroborated the positive charge of the liposomes containing ICG (+60 mV). The incorporation efficiency (IE%) of ICG into the liposomes was 40% and the final formulation did not change the physicochemical properties of liposomes (Figure 1E; and Figure S1, Supporting Information). To compare the optical properties of the liposome-ICG with free ICG and DiR in DMSO, as a standard procedure for cell labeling, the optical density (OD) was studied (Figure 1F). At the same concentration of dye ($80 \times 10^{-6} \text{ M}$), liposome-ICG in 5% dextrose (solid line, $\lambda = 810 \text{ nm}$), and DiR in DMSO (dashed line, $\lambda = 755 \text{ nm}$) displayed identical OD at 22. For the free ICG in dextrose, the OD at 780 nm was 15, lower than the same amount incorporated into liposomes, confirming its better stability within liposomes as previously reported.^[14] The OD overtime (Figure 1G) confirmed high stability for liposome-ICG in dextrose and DiR in DMSO, while the optical properties for ICG in dextrose disappear after 5 d.

Liposomes represent a class of nanoparticles with unleashed potential in the landscape of nanoparticle-based development of labeling agent for cell tracking in vivo. Formulations of liposome-ICG have been reported to enable the study of the lymphatic function during tumor progression,^[15] as well as combinatorial chemotherapy and photothermal therapy for cancer treatment.^[11] Liposomes are primarily constituted of lipids and therefore perfectly biocompatible and biodegradable within the human body. Gadolinium-diethylenetriamine pentaacetic acid (Gd-DTPA) loaded liposomes have been reported for labeling and tracking of mesenchymal stem cells using MRI.^[16] The liposome-ICG nanoprobe design presented here is based on a positively charged lipidic composition, given the cationic contribution of DOTAP to the overall surface charge of the system. The positive charge on the surface of the system promotes the interaction with the moderately negatively charged surface of cells enabling cellular uptake. The organic,

biocompatible, and biodegradable composition of liposomes circumvent the controversial argument of ion-induced toxicity linked to the use of heavy metals and radiotracers employed in the composition of contrast agents connected to the use of imaging modalities based on ionizing sources, such as MRI, PET, and SPECT.^[17]

Stability of Liposome-ICG Nanoprobes in Cell Media: To test their suitability as nanoprobes for cell labeling, the OD over 24 h of plain liposomes, DiR, ICG, and liposome-ICG was measured in 5% dextrose, Phosphate Buffered Saline (PBS), Minimum Essential Media (MEM), and Dulbecco's Modified Eagle's Medium (DMEM) (Figure 2). In all conditions tested, the peak at 755 nm for the DiR disappears literally and a broadband is observed. The ICG keeps its optical properties only in dextrose but not in the high electrolyte content media such as PBS, MEM, and DMEM. Liposome-ICG was the best candidate for further studies due to its higher and more stable optical properties in all conditions tested.

ICG has recently been reported as able to label human embryonic stem-cell derived cardiomyocytes,^[18] monocytes,^[19] and placental mesenchymal stem cells.^[20] Interestingly, the ICG doses used for cell labeling in all of these studies were at least one order of magnitude higher than the concentrations used in our study. This observation allows us to make an important consideration: the optical properties of the dye in all the media are clearly affected, as shown in Figure 2 and Figure S2 (Supporting Information), most likely as a result of the poor solubility. Although high amounts of dye are present in the labeling solutions, only a fraction is interacting superficially with the cell membrane, making the reported labeling procedure with ICG transient and prone to variations. Indeed, Christensen et al. have reported that consecutive washing and centrifugation steps cause a gradual decrease in the fluorescence of labeled monocyte cells and a return to baseline conditions in only 12 h. Direct labeling of cells using these high concentrations of ICG seems to result also in a short-term labeling effect: tracking of labeled monocytes was achieved up to 24 h.^[19]

Cell Labeling: Liposome-ICG nanoprobes were tested for their ability to label cells on different cell lines, including cancer cell lines, such as A549 lung epithelial cancer cells, HT-29 colon cancer cells, and U87 MG glioblastoma cells. Confocal microscopy confirmed that all cell lines were positive for ICG labeling upon incubation with liposome-ICG, at DOTAP:Chol and ICG concentrations of $0.2 \times 10^{-3} \text{ M} : 0.1 \times 10^{-3} \text{ M}$ and $8 \times 10^{-6} \text{ M}$, respectively (Figure 3A).

U87-MG labeled cells were compared for duration of fluorescence signal to control labeled cells with ICG dye alone (negative control) and DiR dye alone (positive control). DiR is a commercial dye conventionally used for the staining of cell membranes with absorption and emission spectra in the same NIR region as ICG. Labeling of cell membrane with DiR is a good method for in vitro investigation under fluorescent microscopy as it gives rise to a strong and homogeneous signal. The disadvantage of labeling cells with DiR for in vivo cell tracking lies in the fact that the fluorescence of the dye is soon lost over time: at the tested concentration, while we could achieve a good and homogeneous staining of cell membrane after 8 h upon incubation with DiR, the fluorescence signal was lost already after 24 h (Figure 3B, top panel). In a recent

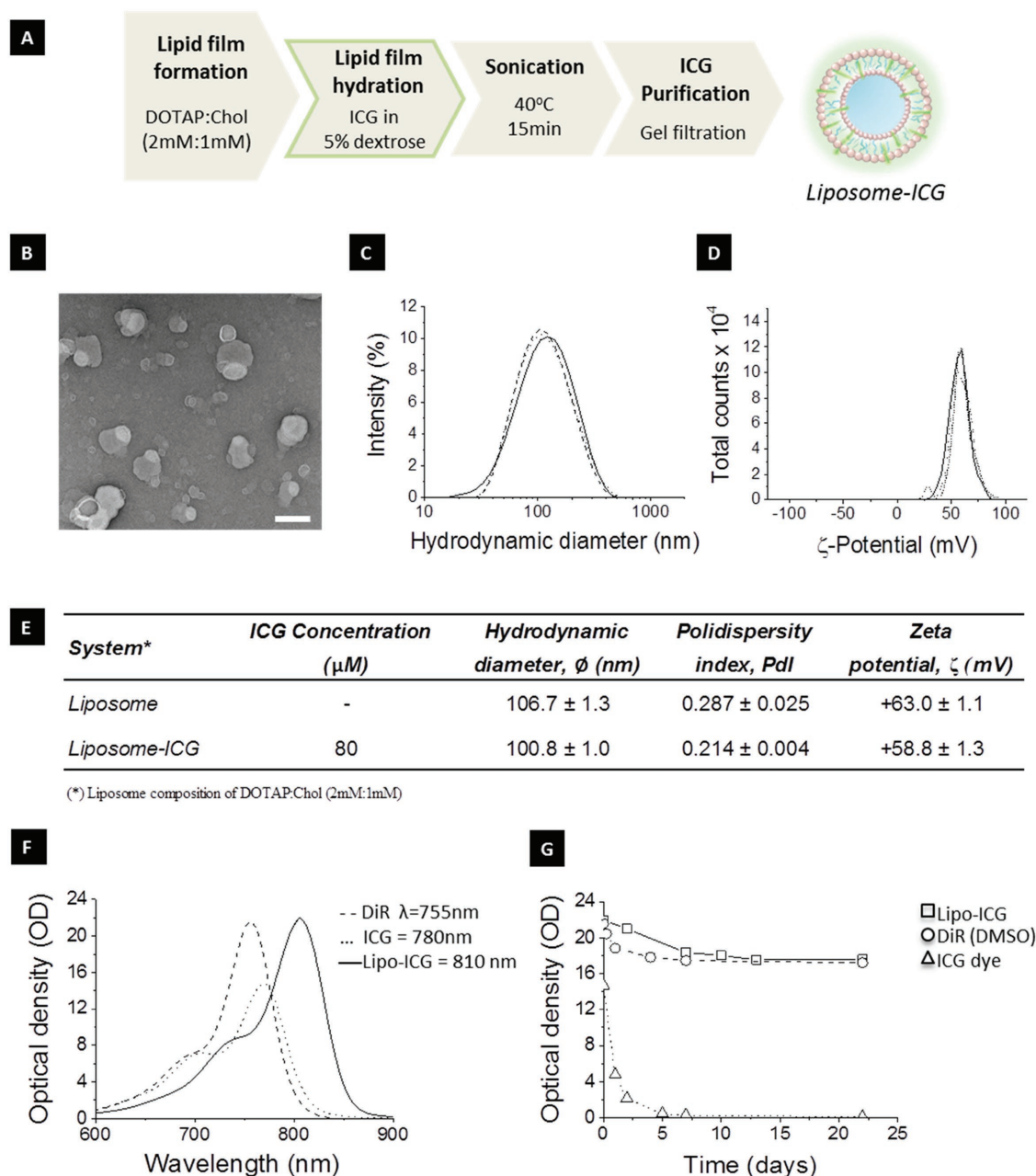


Figure 1. Cationic liposomal indocyanine green engineering and characterization. A) Schematic depiction of the protocol used for the incorporation of ICG in cationic liposomes DOTAP:Chol ($2 \times 10^{-3} \text{ M} : 1 \times 10^{-3} \text{ M}$). B) TEM micrograph of the liposome-ICG (scale bar 200 nm). C) Hydrodynamic diameter and D) ζ -potential measurements of liposome-ICG. E) Table summarizing the physico-chemical properties of plain liposomes compared to liposomes incorporating ICG. F) Optical density (OD) spectra on the day of preparation and G) maximum OD overtime of cationic liposome-ICG in 5% dextrose (squares), DiR in DMSO (circles), and ICG in 5% dextrose (up-triangles), at DiR and ICG concentrations of $80 \times 10^{-6} \text{ M}$.

study, Ruan et al. used labeling of embryonic stem cells (ES) with DiR as a mean to track ES after intravenous injection: the data reported show that cells were detected up to 24 h postinjection, but no further data on fluorescence at later time points were reported in the study.^[21] ICG is the only NIR dye FDA-approved, with poor optical properties overtime in cell media, as shown in Figure S2 (Supporting Information), therefore at the concentration tested in this study cell labeling did not occur by simply incubating cells with ICG dye alone (Figure 3B,

central panel). Only cells labeled using the liposome-ICG nanoprobes demonstrated efficient labeling over time (Figure 3B, bottom panel).

Labeling of hMSC and In Vitro Toxicity: To elucidate the concept of cell labeling for in vivo tracking hMSC were labeled with liposome-ICG nanoprobes. Cells that are not fully differentiated at the time of transplantation may present some risks for the patient relatively to malignant transformation, graft-versus-host disease, and graft failure or organ damage.

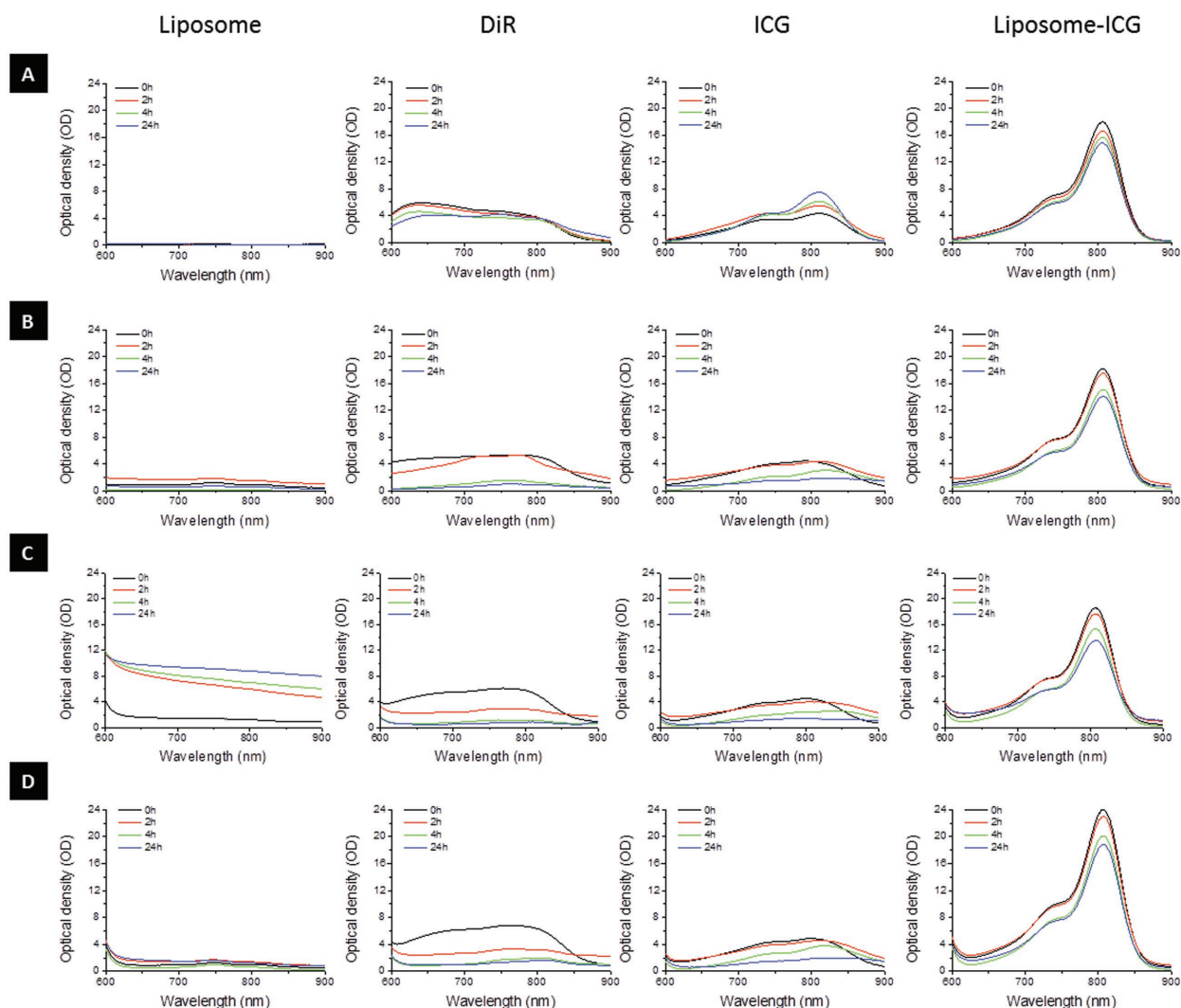


Figure 2. Optical density of plain liposomes, DiR, ICG, and liposome-ICG in A) 5% dextrose, B) PBS, C) MEM, and D) DMEM media at 0 h (black lines), 2 h (red lines), 4 h (green lines), and 24 h (blue lines). DiR and ICG concentrations of 80×10^{-6} M.

OptiMEM was used in the present study for the subculture of hMSC due to the poor OD stability of liposome-ICG in MesenPRO over 4 h (Figure S3, Supporting Information), the media used for the subculture of hMSC.^[22] For this reason, cell labeling was performed using OptiMEM: after allowing the liposome-ICG nanoprobe to interact with the cells for 2 h in OptiMEM, cells were washed with PBS, and subculture resumed with MesenPRO. Cationic liposomes were chosen to confer a rapid cellular uptake, therefore a toxicity dose-response assay was needed to identify the ideal concentration able to provide efficient labeling while circumventing any cytotoxicity for the cells related to the cationic nature of the liposomes. The lactate-dehydrogenase LDH assay was used for the purpose, as the enzyme LDH is released from the cells as a consequence of cell membrane permeabilization caused by cationic materials. As shown in **Figure 4A**, 24 h after transfection hMSC treated with increasing ICG concentrations into liposomes, from 0.8 to 2.6 μm , maintained cell viability, and cell survival was not different from that of untreated cells. At

the ICG concentration of 4 μm , more than 50% of cells died. Similarly, cell viability decreased to about 50% with 4 μm of ICG when we measured the conversion of 3-(4,5-dimethylthiazol-2-yl)-2,5-diphenyltetrazolium bromide (MTT) in insoluble formazan crystals to assess mitochondrial metabolism (Figure 4B), as ICG has been reported to have a modest toxic effect on mitochondrial metabolism.^[23] We performed all of our further labeling experiments using 2 μm ICG concentration where cells remained viable and were able to efficiently uptake liposome-ICG nanoprobe (Figure 4D). Flow cytometry confirmed that virtually all cells were positively labeled with liposome-ICG nanoprobe (Figure 4C) and we could measure a linear increase of the fluorescence using the whole-body imaging camera by increasing the number of cells exposed to the liposome-ICG nanoprobe in vitro (Figure S4, Supporting Information).

Following the labeling procedure, hMSC were cultured to form spheroids, as reported.^[22] Mature spheroids were obtained after 5 d of subculture. The very low rate of cell division in

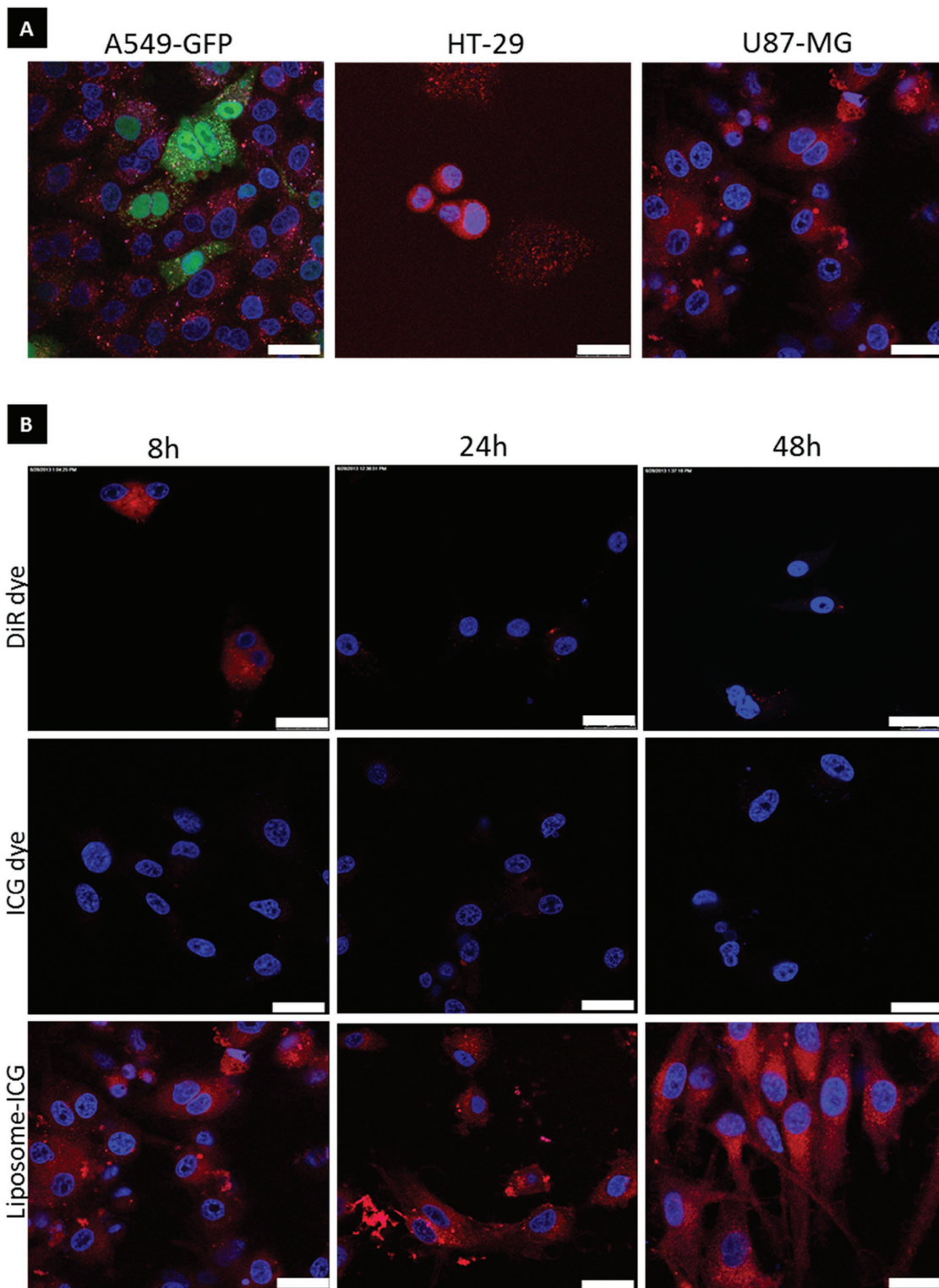


Figure 3. A) Confocal microscopy of different cell lines labeled with liposome-ICG at an ICG concentration of 8×10^{-6} M. B) Labeling of U87 MG with DiR dye (positive control), ICG dye (negative control and liposome-ICG nanoprobe) (scale bar = 25 μ m; Blue = DAPI nuclear staining, Red = dye staining; Green = green fluorescent protein (GFP)).

the spheroids minimized the risk of signal dilution that may occur with cell division. hMSC labeled as monolayers were able to form homogeneously labeled spheroids, as measured using

fluorescence imaging (Figure 4E–G). Fluorescence light microscopy revealed the cellular organization of the spheroids, with a bright fluorescent signal at cellular level which was confirmed

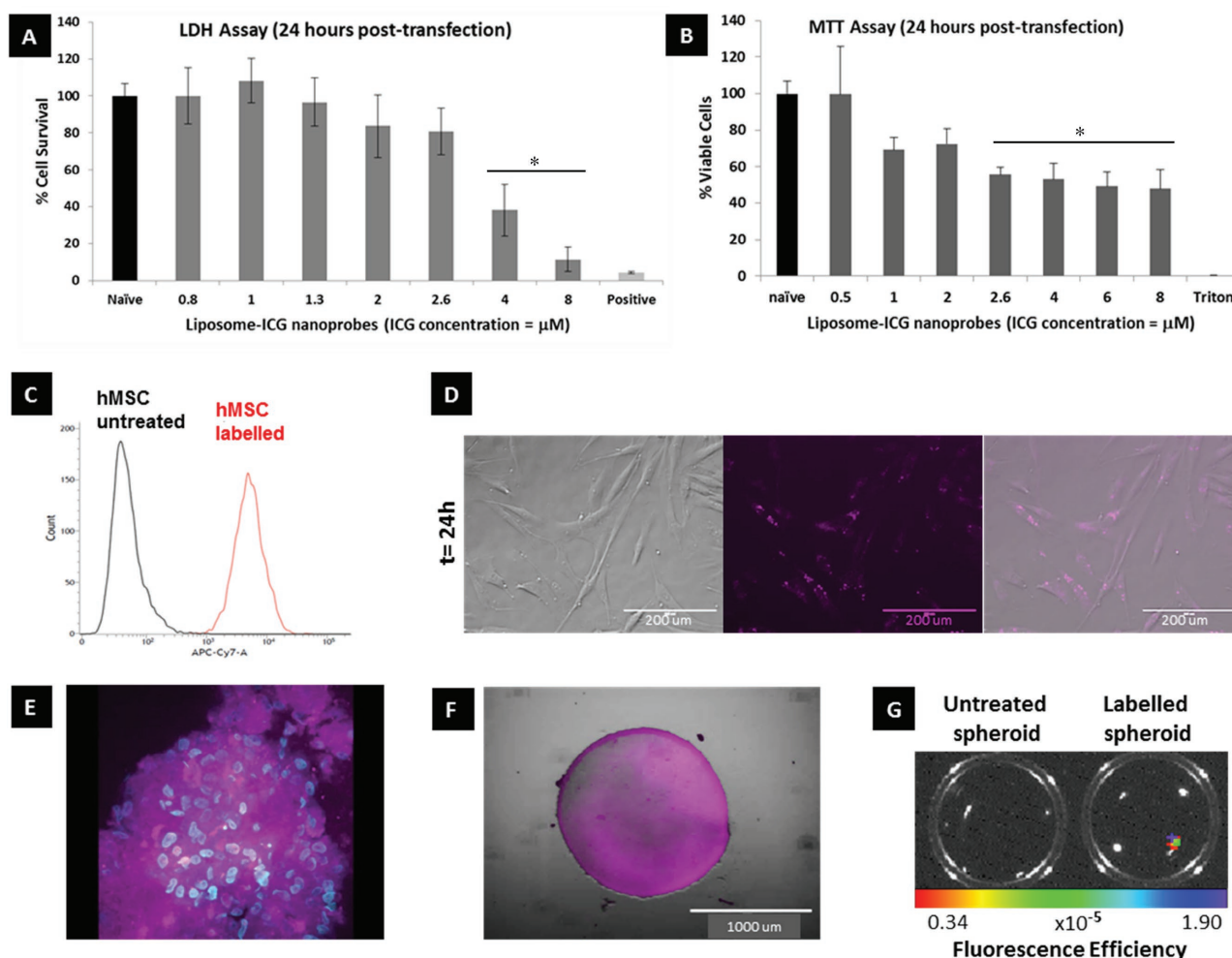


Figure 4. Liposome-ICG nanoprobe labeling hMSC. A) LDH assay on hMSC cells 24 h after labeling with Liposome-ICG at various ICG concentrations (data are presented as mean \pm SEM, $n = 6$ wells, P -values are calculated using one-way ANOVA with Bonferroni correction, $*P < 0.0001$). B) MTT assay on hMSC cells 24 h after labeling with Liposome-ICG at various ICG concentrations. Data are presented as mean \pm SEM, $n = 6$ wells, P -values are calculated using one-way ANOVA with Bonferroni correction, $*P < 0.0001$). C) Flow cytometry profiles of hMSC cells after labeling with Liposome-ICG. D) Labeling of hMSC: epi-fluorescence microscopy of live cells incubated for 2 h with a final ICG concentration of 2×10^{-6} M and imaged after 24 h (scale bar = 200 μ m; Positive labeling of the cells via ICG-liposome nanoprobe is rendered with magenta false coloring). E–G) Epi-fluorescence pictures of hMSC labeled spheroids (60 000 cells) obtained using E) confocal microscopy (Z-stack Maximum Intensity Projection) to achieve cellular level resolution, F) an EVOS epi-fluorescent microscope for live cell imaging (scale bar 1000 μ m), G) an IVIS Lumina II camera.

by a strong fluorescence signal also under the FLI camera (also used for whole body imaging), with excitation at 745 nm.

In Vivo Tracking of Labeled hMSC Spheroids: The efficiency of the liposome-ICG nanoprobe to be used as a way to label hMSC for in vivo cell tracking was tested by transplanting the spheroids in different tissues, hence at different depths. For subcutaneous administration, 15 labeled spheroids (8000 cells/spheroid) were injected in the right flank of athymic nude mice. Fluorescence images were acquired from 24 h to 3 weeks after injection (Figure 5B; and Figure S5, Supporting Information). Fluorescence, while decreasing overtime, was detectable throughout 2 weeks in all transplanted animals (Figure 5C). Residual fluorescence signal arising from the labeled cells was still detected in some animals after 3 weeks (Figure S5, Supporting Information).

For intracranial administration, athymic nude mice were stereotactically injected in the right striatum with 5 spheroids

(8000 cells/spheroid), as transplanting 15 spheroids would have increased considerably the intraparenchymal pressure. Although fewer spheroids could be delivered in this tissue, in comparison to subcutaneous administration, the fluorescence signal of the labeled cells was sufficient to be recorded through the skull in living animals up to 1 week (Figure 5B). At this tissue depth, cells could only be imaged at 2 weeks in the brain ex vivo. Fluorescence images were acquired from 24 h to 21 d after engraftment (Figure 5B; and Figure S5, Supporting Information). Fluorescence was detected for 14 d in all transplanted animals. After 21 d cells could still be tracked in some of the transplanted animals (Figure S5, Supporting Information).

To the best of our knowledge, for the first time, transplanted stem cells were imaged in situ after engraftment deep in the brain up to 1 week in living animals without recurring to imaging techniques based on ionizing sources and without the

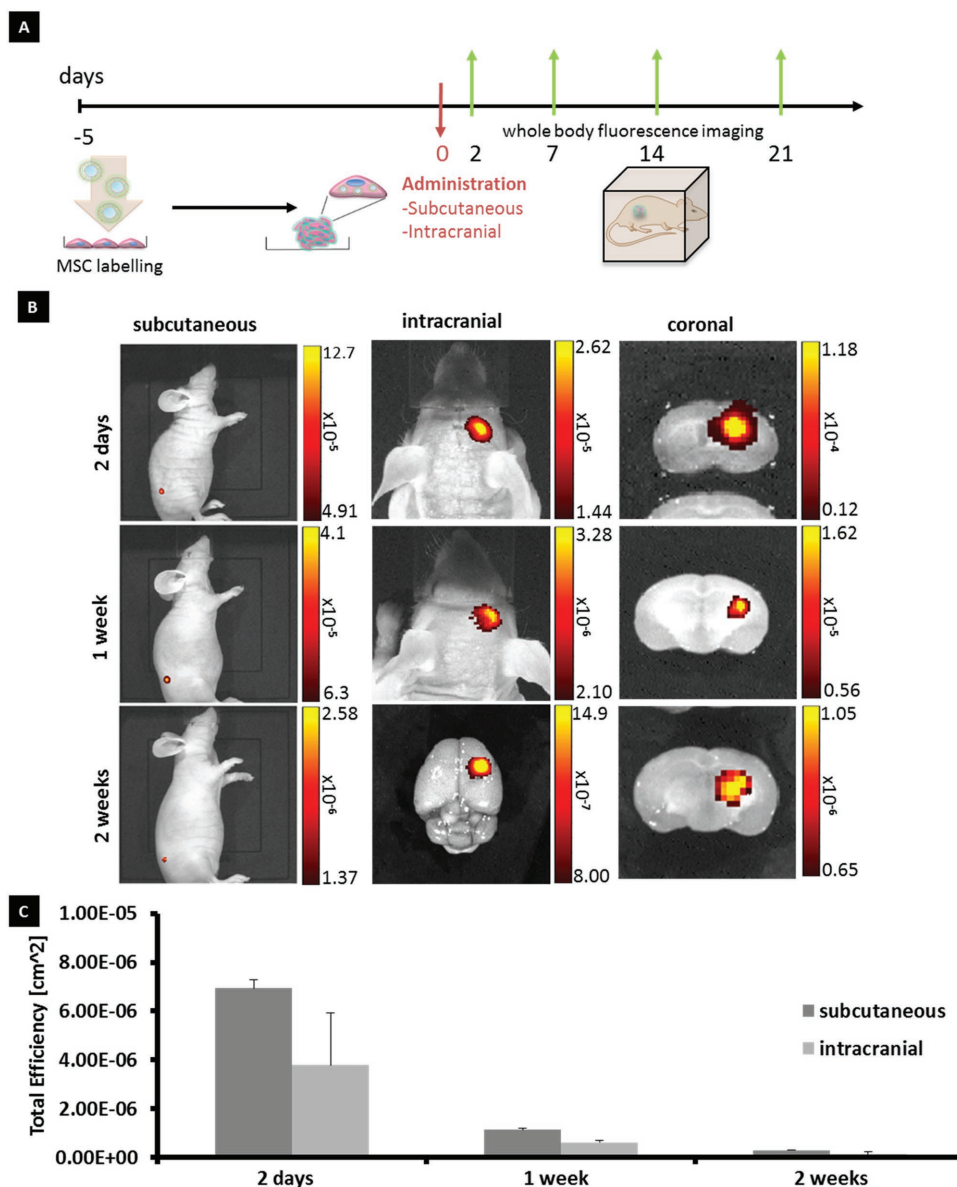


Figure 5. hMSC tracking overtime in vivo. A) In vivo experiment design. B) Tracking of labeled hMSC in living animals (2 replicates of $n = 3$): subcutaneous administration (left panel) of 15 spheroids and intracranial administration (central and right panels) of 5 spheroids (8000 cells/spheroid). C) Quantification of fluorescence intensity in regions-of-interest (ROI) expressed as total efficiency \pm standard deviation.

need to genetically modify the cells. The development of safe nanoprobes to be used in conjunction to imaging techniques based on nonionizing sources is highly desirable. It is widespread opinion that imaging should be a complementary tool to incorporate in more studies of stem cell transplantation.^[3,24]

In recent years, nanoparticles of various chemical compositions have been developed in an effort to improve the efficiency of labeling agents for cell tracking in vivo. Nanoparticle-based labeling agents have been previously reported to have prolonged intracellular retention in comparison to small molecule dyes.^[25] The cationic nature of liposome-ICG favors cellular internalization, thus giving rise to a labeling protocol rapid and efficient, in comparison to coated nanoparticles of various chemistry,^[26,27] that have low rate of internalization and require

overnight or 24 h incubation. More sophisticated systems based on semiconducting polymers (SNPs) have shown that rapid labeling is achievable: Pu et al. have reported that efficient labeling of renal carcinoma cells with NIR-SNPs permitted cell tracking of 1×10^6 labeled cells implanted subcutaneously in mice for a period of 12 d with a decrease of the signal of about $35 \pm 9.5\%$.^[8] In our study, the number of hMSC cells implanted subcutaneously was nearly one order of magnitude smaller (1.2×10^5 cells), nevertheless the signal was detected for up to 21 d.

Recently, hybrids of polymeric nanoparticles conjugated quantum dots, decorated with the cell-penetrating peptide derived from HIV-1, have been reported as labeling agents for mesenchymal stem cells.^[7] In vivo tracking of 1×10^6 labeled

cells allowed for live imaging up to 21 d of the cells implanted subcutaneously. This tracking window is comparable to our results, where the signal endured for up to 21 d for some of the transplanted mice. However it is important to note that tracking systems based on quantum dots suffer from potential degradation caused by reactive oxygen species with high risk of release of heavy metal ions.^[28] The advantage of the liposome-ICG nanoprobe lies on the safe profile of the carrier toward the human host and on the safety profile of the imaging modality (NIR optical imaging) that would allow for consecutive imaging sessions in a short temporal window to follow the fate of transplanted cells. These data prove that liposome-ICG nanoprobe holds great promises as labeling agent for deep tissue imaging and long-term cell tracking in living animals.

We have developed liposome-ICG nanoprobe as a rapid, efficient, and durable cell labeling agent. Labeled cells retained viability and were able to form spheroids, as previously reported.^[22] It is clear that cell-based therapies can offer alternatives to treatment of various diseases. However, more precise information on their fate following grafting within the host tissues and distribution throughout the body is necessary. Liposome-ICG nanoprobe enables real time noninvasive *in vivo* cell imaging to follow engraftment and fate of cells following transplantation by means of a safe imaging modality, NIR optical imaging, and therefore have the potential to be used as a tool to better understand stem cell fate upon transplantation that can provide important insight for the development of stem cell-based therapies. Combining this novel technology platform with advanced optical imaging techniques such as fluorescence molecular tomography coupled to computed tomography or multispectral optoacoustic tomography may have the potential to provide a thorough assessment of the biodistribution and fate of labeled cells following transplantation, as these techniques would enable more precise localization deep in the tissues overcoming the limitations of 2D imaging.

Experimental Section

Engineering and Characterization of Cationic Liposomal Indocyanine Green (Liposome-ICG): Liposomal ICG formulations were prepared using the lipid film hydration method. 1,2-dioleoyl-3-trimethylammonium-propane hydrochloride (DOTAP, Lipoid, Germany) and cholesterol (Chol, Avanti Polar Lipids, USA) were dissolved in chloroform/methanol (4:1, v/v) and the organic solvents were evaporated using a rotary evaporator for 30 min at 40 °C. The resulting thin lipid film was hydrated in 5% dextrose containing 200×10^{-6} M Indocyanine Green (ICG, Pulsion Medical Systems, Germany). The dispersion was bath sonicated (VWR USC300DF, 80 W) for 15 min at 40 °C and remained at room temperature for 30 min to stabilize the colloidal system. The free ICG was removed by eluting the sample through a spin desalting column (ThermoFisher, Zeba Spin Desalting Column, 7 K MWCO, 5 mL) and then centrifuging at room temperature for 5 min at 2000 rpm. The ICG incorporation efficiency (IE%) was determined by UV-vis spectroscopy in a Varian Cary WinUV 50 Bio spectrophotometer (USA) after diluting the sample 50 times in DMSO and vortexing for few seconds to make sure the liposomes were completely broken, the final incorporation efficiency was calculated using the equation $IE\% = [\text{Incorporated ICG Concentration}/\text{Initial ICG Concentration}] \times 100$. TEM micrograph was performed with a Tecnai 12 instrument operated at 120 kV accelerating voltage. Particle diameter was measured at 25 ± 0.1 °C by a Nano ZS series HT (Malvern, UK) in back scattering mode, at 173° and

$\lambda = 632.8$ nm. For electrophoretic mobility (μ) measurements the same dispersions were placed into U-shaped cuvettes, equipped with gold electrodes. The ζ -potential is related to the μ by Henry's equation valid in the Smoluchowski approximation, when the screening length is much smaller than the particle radius. Optical stability studies for the liposomal ICG formulation in 5% dextrose was followed over 22 d in a Varian Cary winUV 50 Bio spectrophotometer (USA).

Confocal Imaging of Labeled Cells: A549-GFP, HT-29, and U87MG cells were, respectively, cultured according to ATCC subculturing specifications (<http://www.lgcstandards-atcc.org/>). 5000 cells per well were seeded onto Millicell EZ slides (Millipore) eight-well glass chambers and left to adhere overnight. Cells were washed with PBS, then exposed to $8 \mu\text{m}$ of ICG concentration into liposomes containing 0.2×10^{-3} M DOTAP and 0.1×10^{-3} M Chol, or controls of plain liposomes, DiR or ICG dye alone, diluted in serum free cell media. After 4 h incubation cells were washed twice with PBS, fixed with 4% PFA for 10 min. Slides were mounted with Vectashield medium containing DAPI (Vector Laboratories) to stain the cell nuclei. Images were acquired on a Leica TCS SP8 Mp-OPO microscope used in confocal mode with HyD detectors.

hMSC Labeling and Spheroid Culture: hMSCs were cultured as previously described by Ball et al.^[22] Briefly, Human bone marrow-derived mesenchymal stromal cells from a 21-year-old female and 33-year-old males (Lonza), were cultured using MesenPRO RS medium (Life Technologies) supplemented with 1% L-glutamine and 1% Penicillin/Streptomycin. Cells were cultured as a monolayer up to passage 5, then washed with PBS, incubated for 2 h with liposome-ICG at DOTAP and ICG concentrations of 50 and $2 \mu\text{m}$, respectively, and washed with PBS. Spheroids were formed by seeding 8000 labeled hMSC into individual wells of a low adhesion round bottomed 96-well plate and cultured at 37 °C for 5 d before transplantation.

LDH Assay: hMSC cells were seeded in a 96-well plate at a density of 5000 cells/well and cultured until they reached 80% confluence. Liposome-ICG treatment groups ($n = 6$) were as follows: 0.8×10^{-6} , 1×10^{-6} , 1.3×10^{-6} , 2×10^{-6} , 2.6×10^{-6} , 4×10^{-6} , and 8×10^{-6} M ICG concentrations. LDH enzyme release was measured using the CytoTox 96 nonradioactive cytotoxicity assay (Promega) following manufacturer instructions. Media were sampled 24 h after treatment and normalized with 1% Triton X-100-treated positive control representing 100% LDH release.

MTT Assay: hMSC were seeded in a 96-well plate and cultured to reach 80% confluence. Liposome-ICG treatment groups ($n = 5$) were as follows: 0.8×10^{-6} , 1×10^{-6} , 1.3×10^{-6} , 2×10^{-6} , 2.6×10^{-6} , 4×10^{-6} , and 8×10^{-6} M ICG concentrations. Triton 0.1 mg mL⁻¹ was used as positive control. After 4 h cells were washed with PBS and fresh culturing media was added to the cells and these were allowed to grow further 20 h. Then cells were washed with PBS and 100 μL of MTT diluted in culturing media was added (1:10 v/v; MTT original stock 5 mg mL⁻¹). Cells were incubated for 3 h and formazan crystals solubilized with 100 μL of DMSO for 15 min at 37 °C. The absorbance was measured in a microplate reader (FluoSTAR, Omega) and cell viability calculated as (Absorbance of treated cells/Absorbance of control cells) * 100.

Flow Cytometry of Labeled Cells: hMSC cells (passage 5) were seeded in 6-well plates and allowed to reach 80% confluence. After incubation with Liposome-ICG at a concentration of ICG of $2 \mu\text{m}$ for 2 h in Optimum, cells were washed with PBS and medium changed with MesenPRO RS. Cells were further cultured up to 24 h, then trypsinized and centrifuged. The cell pellets were collected and suspended in MesenPRO RS. The fluorescence was measured immediately by flow cytometry using a FACSVerser (Becton Dickinson) with the APC-Cy7 detection channel.

Imaging of Labeled hMSC Spheroids: Fixed labeled spheroids were imaged at cellular level using an inverted Leica SP5 microscope with equipped with HyD detectors. Live imaging of labeled spheroids was performed using an EVOS FL Cell Imaging System equipped with a Cy7 LED light cube. Spheroids seeded on a black 96-well plate were imaged using an IVIS imaging camera with excitation at 745 nm and emission filter set at 700–840 nm.

hMSC *In Vivo* Transplantation: All experiments were performed in accordance with the approved recommendations and policies of the UK

Home Office (Animal Scientific Procedures Act 1986, UK). Male athymic nude Fox1nu weighing 20–24 g (4–6 weeks old Harlan, UK) were housed in IVC cages in number of four animals per cage. Animals were left to acclimatize 1 week before entering in the experiment and food and water was provided ad libitum.

Prior surgery anesthesia was induced by inhalation of isoflurane.

Subcutaneous Transplantation: Animals (2 replicates of $n = 3$) received a subcutaneous injection of 15 spheroids (8000 cells/spheroid) on the right flank. Imaging was performed after 1, 2, 7, 14 d. Animals ($n = 3$) in the second arm of the experiment were also imaged after 21 d.

Intracranial Transplantation: Animals (2 replicates of $n = 3$) received a stereotactic injection of 5 spheroids (8000 cells/spheroid). The stereotactic coordinates were: 0.1 mm posterior to the bregma, 2.3 mm to the right of the midline and 3 mm below the surface of the brain to target the caudate–putamen area of the brain. During surgical procedures, the animals were oxygenated and heated to ensure a 37 °C rectal temperature. After recovery, the animals were returned to their cages. Imaging was performed after 1, 2, 7, 14 d. Animals ($n = 3$) in the second arm of the experiment were also imaged after 21 d.

IVIS Imaging: The fluorescence signal from the cells labeled with liposome-ICG nanoprobe in the brain and in the right flank of the animals was measured using an IVIS Lumina Fluorescent imager (Perkin Elmer) with excitation at 745 nm and emission filter sets 700–840 nm.

Statistical Analysis: GraphPad Prism 6 was used for statistical analysis. LDH and MTT assays data are presented as mean \pm SD, samples ($n = 6$ wells) were analyzed using one-way ANOVA with Bonferroni posthoc test ($*P < 0.0001$).

Supporting Information

Supporting Information is available from the Wiley Online Library or from the author.

Conflict of Interest

The authors declare no conflict of interest.

Keywords

cell tracking, intracranial, liposomes, mesenchymal stromal cells, spheroids, subcutaneous

Received: March 22, 2017

Revised: June 25, 2017

Published online: August 4, 2017

- [1] E. D. Thomas, H. L. Lochte Jr., J. H. Cannon, O. D. Sahler, J. W. Ferrebee, *J. Clin. Invest.* **1959**, *38*, 1709.
 [2] A. K. Srivastava, J. W. Bulte, *Stem Cell Rev.* **2014**, *10*, 127.
 [3] P. K. Nguyen, J. Riegler, J. C. Wu, *Cell Stem Cell* **2014**, *14*, 431.
 [4] a) M. Hofmann, K. C. Wollert, G. P. Meyer, A. Menke, L. Arseniev, B. Hertenstein, A. Ganser, W. H. Knapp, H. Drexler, *Circulation* **2005**, *117*, 2198; b) W. J. Kang, H. J. Kang, H. S. Kim, J. K. Chung, N. C. Lee, D. S. Lee, *J. Nucl. Med.* **2006**, *47*, 1295; c) R. S. Karpov, S. V. Popov, V. A. Markov, T. E. Suslova, V. V. Ryabov, Y. S. Poponina, A. L. Krylov, S. V. Sazonova, *Bull. Exp. Biol. Med.* **2005**, *140*, 640.

- [5] a) F. Li, R. I. Mahato, *Mol. Pharmaceutics* **2008**, *5*, 407; b) J. Terrovitis, M. Stuber, A. Youssef, S. Preece, M. Leppo, E. Kizana, M. Schar, G. Gerstenblith, R. G. Weiss, E. Marban, M. R. Abraham, *Circulation* **2008**, *117*, 1555.
 [6] A. M. Smith, M. C. Mancini, S. Nie, *Nat. Nanotechnol.* **2009**, *4*, 710.
 [7] G. R. Jin, D. Mao, P. Q. Cai, R. R. Liu, N. Tomczak, J. Liu, X. D. Chen, D. L. Kong, D. Ding, B. Liu, K. Li, *Adv. Funct. Mater.* **2015**, *25*, 4263.
 [8] K. Pu, A. J. Shuhendler, M. P. Valta, L. Cui, M. Saar, D. M. Peehl, J. Rao, *Adv. Healthcare Mater.* **2014**, *3*, 1292.
 [9] J. V. Jokerst, M. Thangaraj, P. J. Kempen, R. Sinclair, S. S. Gambhir, *ACS Nano* **2012**, *6*, 5920.
 [10] a) N. Lozano, Z. S. Al-Ahmady, N. S. Beziere, V. Ntziachristos, K. Kostarelos, *Int. J. Pharm.* **2015**, *482*, 2; b) S. Magdassi, S. Bar-David, Y. Friedman-Levi, E. Zigmund, C. Varol, G. Lahat, J. Klausner, S. Eyal, E. Nizri, *Surg. Innovation* **2017**, *24*, 139.
 [11] X. Zhang, N. Li, Y. Liu, B. Ji, Q. Wang, M. Wang, K. Dai, D. Gao, *Nanomedicine* **2016**, *12*, 2019.
 [12] a) R. W. Flower, B. F. Hochheimer, *Invest. Ophthalmol.* **1973**, *12*, 248; b) T. Imai, K. Takahashi, H. Fukura, Y. Morishita, *Anesthesiology* **1997**, *87*, 816; c) C. M. Leevy, C. L. Mendenhall, W. Lesko, M. M. Howard, *J. Clin. Invest.* **1962**, *41*, 1169.
 [13] Z. Cesarz, K. Tamama, *Stem Cells Int.* **2016**, *2016*, 9176357.
 [14] N. Beziere, N. Lozano, A. Nunes, J. Salichs, D. Queiros, K. Kostarelos, V. Ntziachristos, *Biomaterials* **2015**, *37*, 415.
 [15] S. T. Proulx, P. Luciani, S. Derzsi, M. Rinderknecht, V. Mumprecht, J.-C. Leroux, M. Detmar, *Cancer Res.* **2010**, *70*, 7053.
 [16] J. Guenoun, G. A. Koning, G. Doeswijk, L. Bosman, P. A. Wielopolski, G. P. Krestin, M. R. Bernsen, *Cell Transplant.* **2012**, *21*, 191.
 [17] S. Kunjachan, J. Ehling, G. Storm, F. Kiessling, T. Lammers, *Chem. Rev.* **2015**, *115*, 10907.
 [18] S. E. Boddington, T. D. Henning, P. Jha, C. R. Schlieve, L. Mandrussow, D. DeNardo, H. S. Bernstein, C. Ritner, D. Golovko, Y. Lu, S. Zhao, H. E. Daldrup-Link, *Cell Transplant.* **2010**, *19*, 55.
 [19] J. M. Christensen, G. A. Brat, K. E. Johnson, Y. Chen, K. J. Burette, D. S. Cooney, G. Brandacher, W. P. A. Lee, X. Li, J. M. Sacks, *PLoS One* **2013**, *8*, e81430.
 [20] V. Sabapathy, J. Mentam, P. M. Jacob, S. Kumar, *Stem Cells Int.* **2015**, *2015*, 8.
 [21] J. Ruan, H. Song, C. Li, C. Bao, H. Fu, K. Wang, J. Ni, D. Cui, *Theranostics* **2012**, *2*, 618.
 [22] S. G. Ball, J. J. Worthington, A. E. Canfield, C. L. Merry, C. M. Kielty, *Stem Cells* **2014**, *32*, 694.
 [23] R. Narayanan, M. C. Kenney, S. Kamjoo, T. H. Trinh, G. M. Seigel, G. P. Resende, B. D. Kuppermann, *Curr. Eye Res.* **2005**, *30*, 471.
 [24] a) N. G. Kooreman, J. D. Ransohoff, J. C. Wu, *Nat. Mater.* **2014**, *13*, 106; b) K. von der Haar, A. Lavrentieva, F. Stahl, T. Scheper, C. Blume, *Appl. Microbiol. Biotechnol.* **2015**, *99*, 9907.
 [25] C. Xu, D. Miranda-Nieves, J. A. Ankrum, M. E. Matthesen, J. A. Phillips, I. Roes, G. R. Wojtkiewicz, V. Juneja, J. R. Kultima, W. Zhao, P. K. Vemula, C. P. Lin, M. Nahrendorf, J. M. Karp, *Nano Lett.* **2012**, *12*, 4131.
 [26] M. Barrow, A. Taylor, P. Murray, M. J. Rosseinsky, D. J. Adams, *Chem. Soc. Rev.* **2015**, *44*, 6733.
 [27] C. Wu, S. J. Hansen, Q. Hou, J. Yu, M. Zeigler, Y. Jin, D. R. Burnham, J. D. McNeill, J. M. Olson, D. T. Chiu, *Angew. Chem., Int. Ed.* **2011**, *50*, 3430.
 [28] Y. C. Wang, R. Hu, G. M. Lin, I. Roy, K. T. Yong, *ACS Appl. Mater. Interfaces* **2013**, *5*, 2786.